Catalysis Today 147S (2009) S87–S93

Contents lists available at ScienceDirect

Catalysis Today

journal homepage: www.elsevier.com/locate/cattod

Preparation of stainless steel microreactors coated with carbon nanofiber layer: Impact of hydrocarbon and temperature

Lucía Martínez-Latorre [a], Pedro Ruiz-Cebollada [a], Antonio Monzón [b], Enrique García-Bordejé [a,*]

[a] Instituto de Carboquimica (C.S.I.C.), Miguel Luesma Castán 4, 50018 Zaragoza, Spain
[b] Institute of Nanoscience of Aragon, Department of Chemical and Environmental Engineering, University of Zaragoza, 50009 Zaragoza, Spain

ARTICLE INFO

Article history:
Available online 28 July 2009

Keywords:
Carbon nanofibers
Stainless steel microreactors
Hydrocarbon

ABSTRACT

We have coated stainless steel microreactors with a well-adhered layer of carbon nanofibers (CNFs). The CNFs have been grown by decomposition of a hydrocarbon over microreactors previously coated with Ni dispersed on alumina. As hydrocarbon we used both methane and ethane. Other parameters varied herein are the hydrocarbon:H_2 gas composition and the CNF growth temperature. For the same growth temperature, the carbon productivity is higher for ethane than for methane. Remarkably, using ethane as carbon source, the carbon yield increased abruptly for temperatures exceeding 898 K. This is coupled with a less defined morphology and size of nanocarbon materials when temperature increases. Some thicker CNFs with diameters up to 200 nm and some non-fibrous carbonaceous protrusions are present at the highest temperatures. Thus, the microreactor channels resulted plugged and with an uneven surface at growth temperatures higher than 898 K. With ethane at the lowest temperatures (853 and 873 K), the only carbon product present was CNF of diameter smaller than 50 nm. The characterisation of the carbon nanomaterials and growth catalyst shed some light about the relationship between the morphology of carbon species and growth temperature.

1. Introduction

The manufacture of chemicals in catalytic micro-structured reactors (MSR) has become recently a new branch of chemical reaction engineering focusing on process intensification and safety. MSR have high specific surface area in the range of 10,000 to 50,000 $m^2\ m^{-3}$, while conventional reactors have around 100 $m^2\ m^{-3}$, reaching values of 1000 $m^2\ m^{-3}$ in exceptional cases. The small channel diameter (<1 mm) enhances mass and heat transport, enabling isothermal operation, improved selectivity and security [1]. One of the main problems in using MSR for heterogeneously catalyzed reactions is the introduction of the catalyst in the reactor channels. The easiest option would be filling microchannels by catalyst powder, but this leads to high-pressure drop and flow maldistribution, diminishing reactor performance. A better approach is MSR with catalytically active walls. The specific surface area is increased by chemical treatment of the channel walls or by their coating with a porous layer. With their inherent high surface area-to-volume ratio, CNFs provide more catalytic surface area, thereby obtaining sufficient activity per unit volume of microreactor, while maintaining a low fluidic resistance due to their open structure. Unlike metal oxide support, CNFs form aggregates with high surface areas, high mesopore volumes and low tortuosity. This eliminates the internal diffusion limitations by preventing concentration gradients inside the CNF layer. CNFs are especially favourable for fast and highly exothermic gas phase reactions and for sluggish liquid phase reactions [2], because mass/heat transfer limitations are prevented while keeping low-pressure drop. Carbon nanofibers (CNF) and carbon nanotubes (CNT) hold many promises as catalyst support [3]. Nevertheless, CNFs in powder form have some drawbacks such high-pressure drop, plugging and flow maldistribution for fixed bed operation, and agglomeration and difficulty of filtration due to the formation of fines for slurry phase operation. For this reason, CNFs have been attached to different macroscopic supports such as monoliths, filters or foams [4–15]. Silica microreactors have also been coated with carbon nanomaterials such as carbon nanotubes [16,17]. To our knowledge, there is no report of stainless steel microreactors coated with carbon nanomaterials. To be competitive with conventional technology, CNF coating must exhibit some properties such as durability without blistering, uniform thickness for equal flow distribution into the channels, high activity and

* Corresponding author. Tel.: +34 976733977; fax: +34 976733318.
E-mail address: jegarcia@icb.csic.es (E. García-Bordejé).

0920-5861/$ – see front matter © 2009 Elsevier B.V. All rights reserved.
doi:10.1016/j.cattod.2009.07.008

selectivity. The good mechanical stability of CNF inside microchannels is crucial to prevent channel blocking by loose CNFs. Various approaches can be utilised to achieve improved mechanical stability of CNFs upon non-porous and flat surfaces like stainless steel. One of them is to coat the microreactor with a porous ceramic layer to deposit the growth catalyst (e.g. nickel) necessary for growing CNFs. In this work, we study the conditions for the growth of a mechanically resistant layer of carbon nanofibers (CNF) on stainless steel microreactors via catalytic decomposition of hydrocarbon. Previously, we coated the microreactor with a well-adhered layer of γ-alumina on which Ni catalyst was dispersed. We have varied several growth conditions such as type of hydrocarbon, temperature and hydrocarbon:H_2 ratio. After characterisation of CNFs grown on microreactrors we have assessed the impact of these variables on the CNF layer properties.

2. Experimental

The microreactor platelets were supplied by Institut für Mikrotechnik Mainz GmbH. At the bottom of Fig. 1, it is shown a microreactor platelet (14 mm × 52 mm) made out of stainless steel AISI 314. At the top, a preliminary platelet (10 mm × 10 mm) made out of the same material is displayed. These preliminary platelets have channels similar to those of the microreactor platelet. These channels are *quasi hemicylindrical* and their dimensions are 285 μm height and 430 μm width. Preliminary platelets have been used for the optimization of the coating in this work. The main elemental components of the platelet surface determined by SEM-EDX analysis are Fe (60.3 wt.%), Cr (17 wt.%), O (12.4 wt.%), Ni (8.2 wt.%), S (1.1 wt.%) and Si (1.2 wt.%). Prior to coating, the microreactors were calcined under static air at 1073 K during 2 h.

2.1. Pre-coating with alumina and Ni catalyst

The method used to coat the monoliths with alumina is a wet chemical sol–gel method. A sol is prepared by mixing pseudo-boehmite (AlOOH, Pural from Sasol), urea and 0.3 M nitric acid with a weight ratio of 2:1:5. The sol is stirred for 2 h. Likewise, a homogeneous and stable sol is formed. Every channel of the microreactor platelets was filled using a syringe and assisted by the capillary forces exerted by the microchannel walls. Immediately after filling the microchannels with the sol, the channels were flushed with pressurised air to remove part of the sol and leave a very thin alumina layer (∼4 μm thickness). The monoliths coated with the sol were allowed to dry at room temperature during two days. Subsequently, the coated microreactors were calcined in air flow up to 873 K with a ramp of 1 K/min and a dwell time of 1 h. Hence, microreactor channels resulted covered with a well-adhered γ-alumina layer. From the weight of the microreactor platelet before and after the coating, the alumina loading was calculated. This ranged between 0.05 and 0.1 wt.% relative to the microreactor platelet weight.

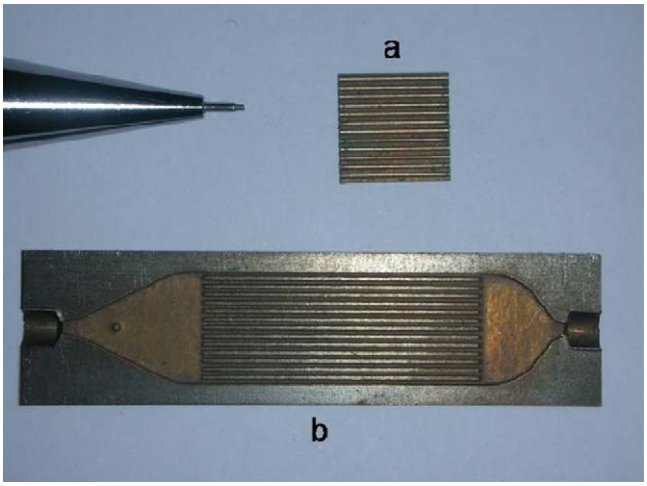

Fig. 1. Microreactor platelets supplied by Institut für Mikrotechnik Mainz GmbH. (a) preliminary platelet used in this work for optimization of the coating; (b) microreactor platelet for catalytic use.

On the γ-alumina coated microreactor, nickel was deposited by strong electrostatic adsorption from a pH-neutral nickel solution. To this end, 29 g $Ni(NO_3)_2{\cdot}6H_2O$ (pure, Sigma–Aldrich), 80 g NH_4NO_3 (pure, Sigma–Aldrich) and 4 ml ammonia solution (25%) were mixed in a 1 l bottle. The microreactor platelet were kept overnight in this solution. Subsequently, microreactor was rinsed thoroughly with deionised water, followed by drying first at room temperature overnight and later at 373 K for 1 h. The microreactors with Ni adsorbed were calcined in flowing nitrogen (1 K/min) up to 873 K followed by a 2 h dwell time. The Ni content in the monoliths was measured by inductive coupled plasma-optical emission spectroscopy (ICP-OES).

2.2. Growth of CNF layer on Ni/alumina coated microreactor

Carbon nanofibers (CNFs) were grown on the as-prepared microreactors platelets. The growth was carried out via catalytic decomposition of methane/hydrogen or ethane/hydrogen gas mixtures, varying gas compositions and temperatures. The reaction was conducted in a horizontal quartz reactor with temperature control (Eurotherm). The gas composition was adjusted with mass flow controllers (Bronkhorst). First, the reduction of the calcined catalyst was carried out in 100 ml/min of a mixture H_2:N_2 (50%) at 823 K for 1 h (heating rate 10 K/min). Then the reactor was heated (10 K/min) to the temperature for CNF growth. Once the temperature was reached, 100 ml/min of hydrocarbon:hydrogen gas mixture was admitted and the reaction was maintained during 3 h. The volumetric ratios of C_2H_6:H_2 used for the growth were 60:40, 50:50 and 40:60. For CH_4:H_2 gas mixtures, we used 90:20 and 80:20 ratios.

2.3. Characterisation techniques

The weight gain after the different stages, i.e. alumina coating and CNF growth, was measured using a balance with a precision up to 1×10^{-3} mg.

SEM analysis was carried out with a microscope SEM EDX Hitachi S-3400 N with variable pressure up to 270 Pa and with an analyzer EDX Röntec XFlash de Si(Li). The images were obtained both from the secondary and backscattered signal.

The adhesion of the coating was tested by drop test in a home-made rig similar to that used by Zapf et al. [18]. The set up consisted of a guided metal block (650 g), which holds the microreactor platelet in the base. This is allowed to fall a distance of 0.5 m, reaching a velocity of 3 m/s when the microreactor impacts into the base platform.

A transmission electron microscopy (TEM) investigation was performed for the CNFs grown on microreactors at different temperatures. A JEOL-2000 FXII electron microscope equipped with a field emission gun was used. Coupled there is a system for energy analysis of dispersed X-rays INCA 200 X-Sight de Oxford Instruments with resolution of 136 eV and 5.9 KeV, which allows the determination of the chemical composition in the focalised micro-region. TEM specimens were prepared by ultrasonic dispersion in ethanol of powder retrieved from the monoliths. A drop of the suspension was applied to a holey carbon support grid.

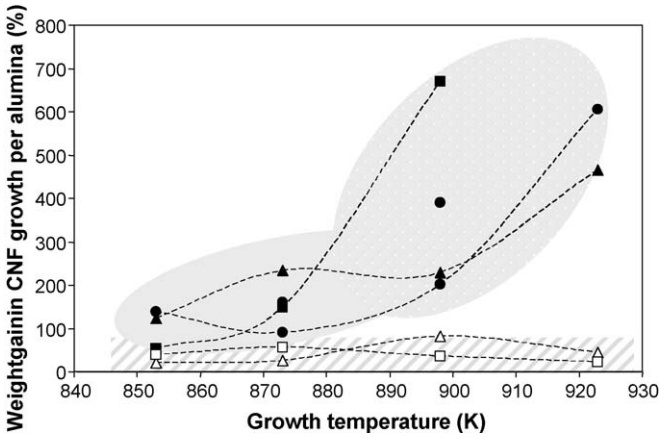

Fig. 2. Weight gain during carbon nanofiber growth relative to alumina coating weight (%) as a function of the growth temperature for three different C_2H_6:H_2 ratios (ml/min:ml/min): (▲) 40:60, (■) 50:50, (●) 60:40, and two different CH_4:H_2 ratios (ml/min:ml/min): (△) 80:20, (□) 90:10. Area solid grey correspond to the experiments with C_2H_6:H_2 while stripped area corresponds to the experiments with CH_4:H_2.

3. Results and discussion

Fig. 2 shows the weight gain after CNF growth on microreactors referred to the weight of γ-alumina coating as a function of the growth temperature both for C_2H_6:H_2 and for CH_4:H_2 gas mixtures with different gas compositions. The carbon yield depends strongly on the hydrocarbon used but does not depend on the hydrocarbon:H_2 ratio. For all the growth temperatures, the carbon yield is higher for ethane than for methane in agreement with the higher reactivity of the former. For methane, the weight gain after carbon growth ranges between 26 and 80 wt.% of the alumina weight and it does not exhibit any dependence with temperature. In contrast, for ethane there is a clear increasing trend of weight gain with temperature for all the gas compositions tested. Two different temperature zones can be distinguished in terms of the slope of the increasing trend. Carbon loading increases only slightly as temperature rises up to around 873 K. In this region, the carbon weight gain ranges from one to two times the alumina weight. In the second region, i.e. at temperatures above 898 K, the carbon yield increases abruptly reaching values up to seven-fold the weight of alumina coating.

We carried out an exhaustive SEM characterisation of the microreactors after the growth at the different temperatures. For the sake of brevity, we only show here the most meaningful images which correspond to the growth with C_2H_6:H_2 at the lowest (853 K) and at the highest temperature (923 K). We omit SEM images of the growth with CH_4:H_2 gas at all the temperatures because they all are comparable to those grown with C_2H_6:H_2 gas at the lowest temperature, i.e. 853 K (Fig. 3).

Fig. 3a–d shows SEM images of CNF coating grown at 853 K with C_2H_6:H_2 gas. Fig. 3a displays that the microchannels are uniformly coated and with a relatively smooth surface. In backscattered top-view image (Fig. 3b), it is apparent that the channels are completely covered by carbon. Fig. 3c and d shows two top-view images of the entangled CNFs taken at two different magnifications. In Fig. 3c, it is possible to envision the pattern of the underlying microreactor surface roughness [19]. The CNFs have uniform diameters smaller than 50 nm (Figs. 3d and 7).

Fig. 4a–d shows SEM images of CNFs coating grown with C_2H_6:H_2 gas mixture at 923 K, i.e. at the highest temperature used. In contrast to the growth at 853 K, the surface of the microchannels is pronouncedly fractured with abundance of carbon protrusions (Fig. 4a and b). The protrusions clog completely some microchannels, thus, rendering the microreactor unsuitable for any purpose. Nevertheless, the major part of the surface is densely forested with CNFs (Fig. 4c). The CNFs grown at this temperature (Fig. 4d) are slightly thicker (50–100 nm) and less entangled than those grown at the lowest temperature (Fig. 3d).

Fig. 5 is a selected SEM image of the microreactor after the growth at 923 K. This image illustrates the three types of carbon nanostructures found throughout all samples examined in this

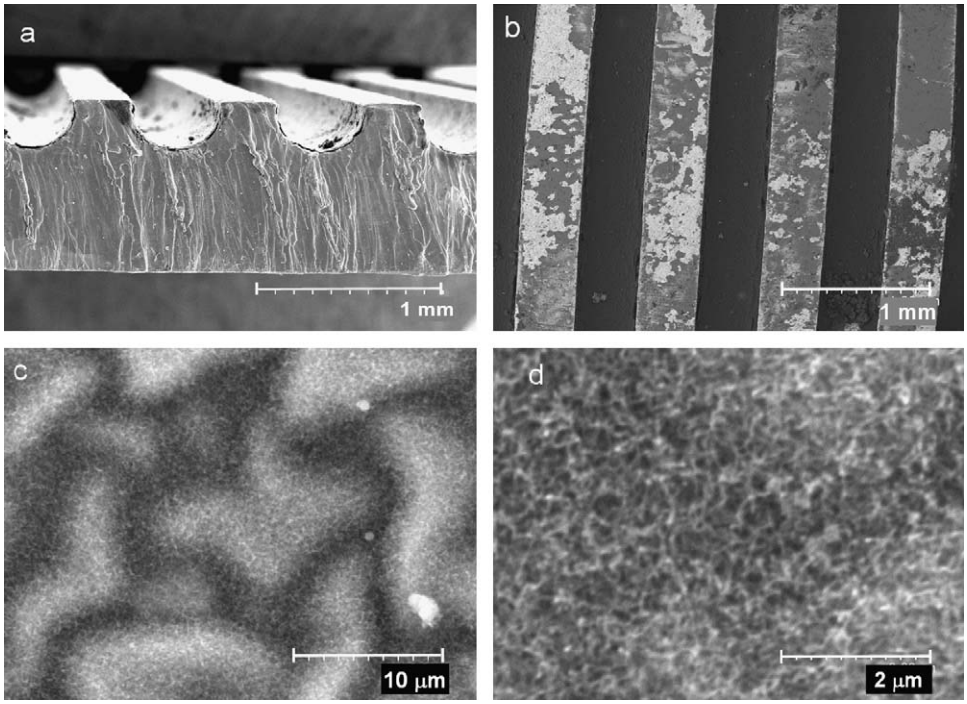

Fig. 3. SEM images of CNF coating grown at 853 K: (a) transversal image recorded with secondary electrons; (b) top-view image recorded with backscattered electrons; (c) high magnification top-view of microchannel surface; (d) high magnification top-view of entangled CNFs.

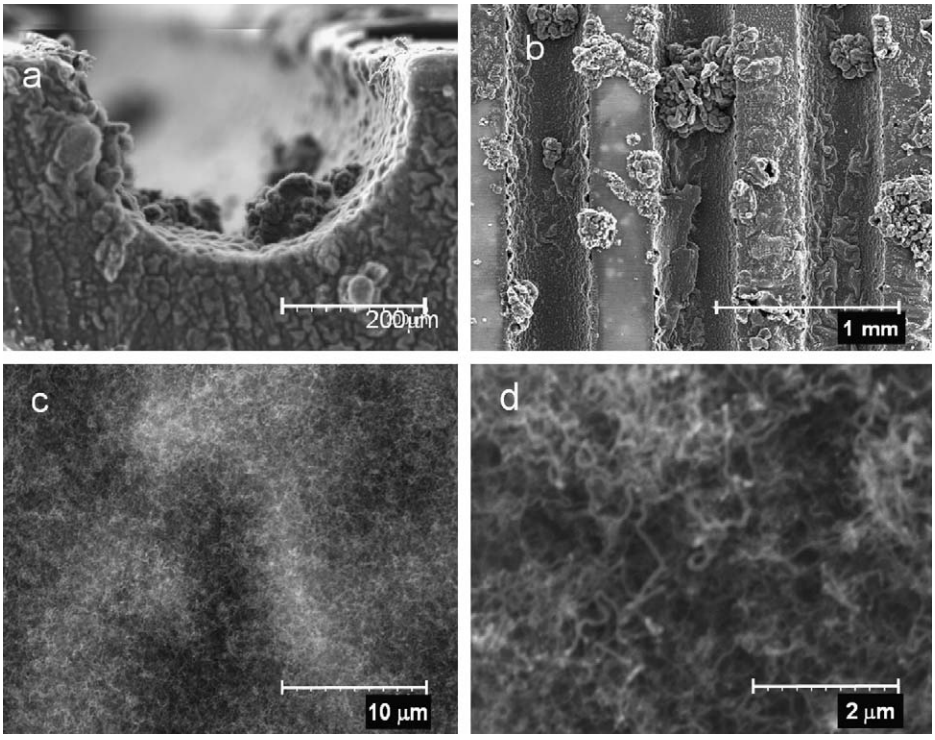

Fig. 4. SEM images of CNF coating grown at 923 K. (a) transversal image of microreactor channels showing some carbon protrusions plugging the channel; (b) top-view of microreactor channels showing a abundant carbon protrusions and fractures; (c) SEM image of a CNF region; (d) magnification of a region with long and thicker CNFs.

work. We classified these types of carbon nanostructures as "thin CNF" with diameters smaller than 50 nm (region 1), "thick CNF" with diameters ranging 80–200 nm (region 2) and "carbon protrusions" (region 3). An in-depth EDX analysis was carried out to all the samples. This enabled us getting insight about the growth catalyst leading to the different carbon nanostructures. All the SEM-EDX results of this work can be summarised in EDX analysis of the different regions in Fig. 5 (Table 1). Fig. 6a and b displays secondary and backscattered SEM images, respectively, of region 1 in Fig. 5, termed as "thin CNF" region. The EDX analysis (Table 1) revealed that the catalyst for the growth of the thin CNFs consisted of Ni. Furthermore, in the backscattered SEM image (Fig. 6b), there is no discernable metal particles pointing out that the growth catalyst is dispersed to very small particle size. TEM-EDS characterisation confirmed that the growth catalyst of thin CNF is Ni and that Ni particle has a mean size of 20 nm (Fig. 7). This size is comparable to the size of Ni catalyst particles dispersed on alumina coated microreactors, as measured by TEM (Fig. 8). Thus, the size of Ni particles is preserved during the CNF growth without significant sintering. The diameter of CNFs resembles the size of the Ni particles (Fig. 7). The "thin CNFs" were grown at all the growth temperatures and they were the only type of carbon nanostructures found when the growth temperature was the lowest (853 K).

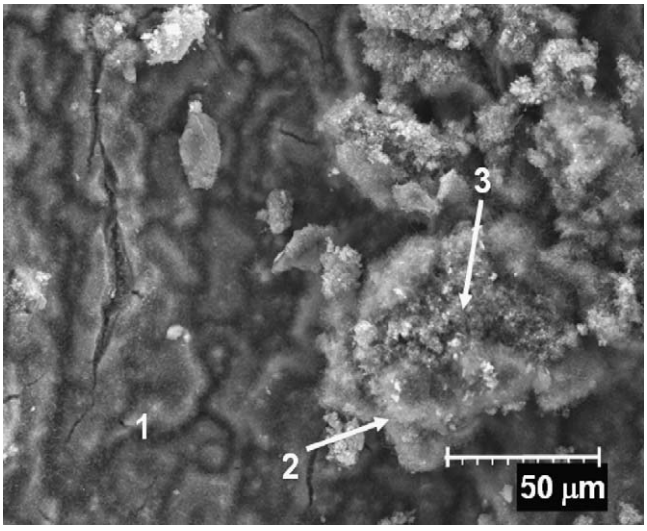

Fig. 5. SEM images of microreactor channel after the growth at 923 K exemplifying the three types of carbon nanostructures observed throughout the examination of all samples. (1) Region of "thin CNFs"; (2) region of "thick CNFs"; (3) region of a "carbon protrusion".

Fig. 9a and b displays magnified SEM images of region 2 in Fig. 5, termed as "thick CNF" area. The EDX analysis (Table 1) revealed that the catalyst leading to the growth of the "thick CNFs" was iron. In contrast to Fig. 6, the catalyst metal particles are larger and, hence, distinguishable in the backscattered SEM image (Fig. 9b). The size of iron particles ranges from 75 to 100 nm. This size is comparable to the diameter of the "thick CNFs". Iron catalyst must come from the microreactor wall because no other source of iron was introduced during the preparation procedure.

The third type of carbon nanostructure has not a filamentous morphology and we have categorised it as "carbon protrusion". SEM images corresponding to region 3 in Fig. 5 is presented in Fig. 10. The EDX analysis (Table 1) disclosed that the catalyst that

Table 1
Normalised composition in weight percentage corresponding to marked area of Figs. 6, 9 and 10 as determined by SEM-EDX after subtracting carbon and alumina.

Figure	Type of carbon material	Fe (wt.%)	Ni (wt.%)	Cr (wt.%)
6	Thin CNF	22.2	74.7	3.0
9	Thick CNF	90.2	5.1	4.7
10	Carbon protrusion	93.1	1.7	5.2

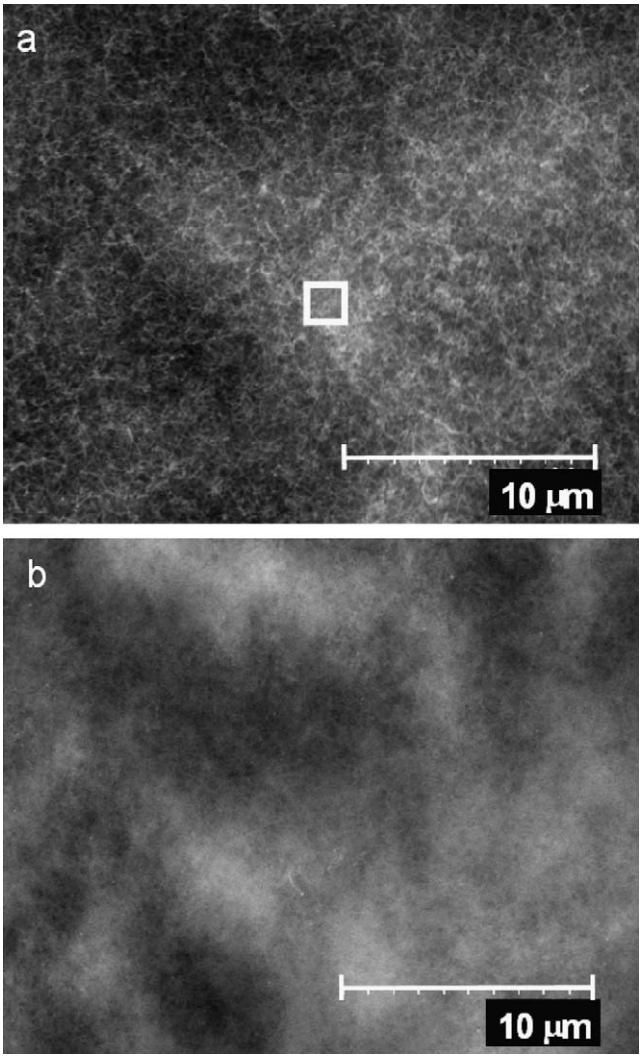

Fig. 6. SEM analysis representative of a region of "thin CNFs" (diameter < 50 nm), which is magnification of spot 1 in Fig. 5. (a) SEM image recorded with secondary electrons; (b) SEM image recorded with backscattered electrons, where no metal particles are visible.

gave rise to carbon protrusions consists also of iron. From the backscattered image (Fig. 10b), we obtained a mean particle size of 150 nm, with several particles having a size of 300 nm and a few reaching up to 600 nm. Thus, the iron particle size is larger and the size distribution broader for the growth of carbon protrusions than for the growth of "thick CNFs" (Fig. 9).

From the extensive SEM characterisation, we evidenced that the growth with CH_4:H_2 gas at all the temperatures and with C_2H_6:H_2 gas at 853 K produced exclusively "thin CNF". For C_2H_6:H_2 gas mixture, when growth temperature is above 873 K, approximately, "thick CNF" and "carbon protrusions" emerge. The presence of the latter is maximised at the highest temperature (923 K). This explains the extremely high weight gain at this growth temperature.

To summarise the results of SEM and TEM, the type of carbon nanostructure is directly linked to the size and nature of active growth catalyst, which is determined indirectly by growth temperature. CNFs of diameter smaller than 50 nm grew from the well dispersed Ni catalyst deposited on the alumina. However, the highest temperatures boosted a process of intensive fragmentation and dusting of iron nanoparticles from microreactor wall. In turn, larger iron particles detached from microreactor, which are inactive at low temperatures, become reactive at higher growth

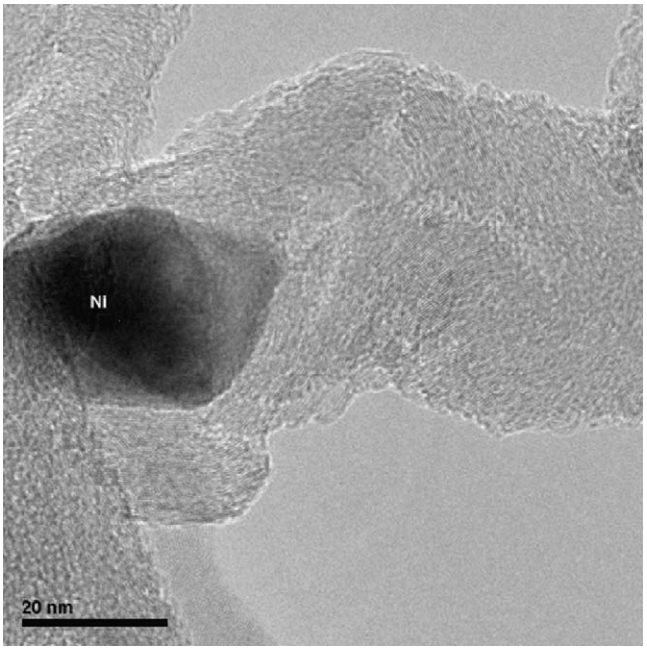

Fig. 7. TEM image of a CNF grown with C_2H_6:H_2 at 853 K. This is a fishbone CNF of 35 nm diameter and a catalyst particle at the tip consisting of Ni as determined by EDX.

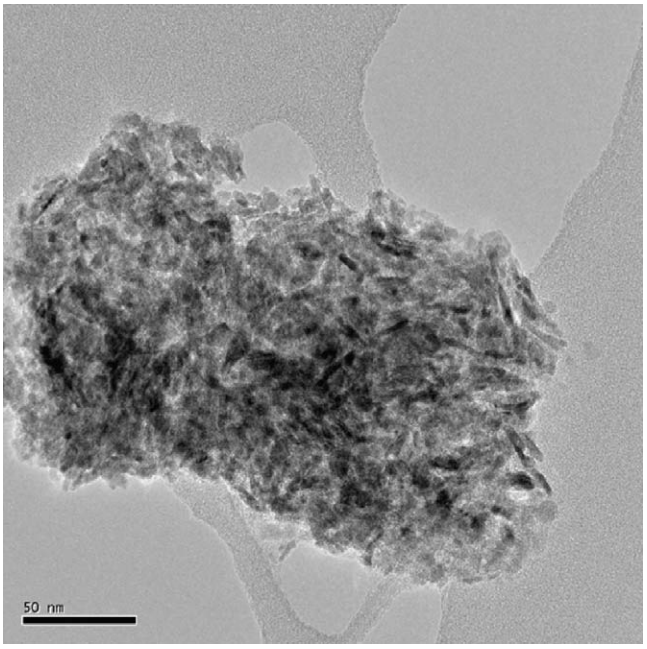

Fig. 8. TEM image of Ni on alumina, which was coated on microreactors. The darkest contrast are Ni particles with average size of 15 nm.

temperatures. The combination of these effects triggered the growth of thicker CNFs (80–200 nm) and carbon protrusions.

The attachment of the CNFs to microreactor platelets was very good with less than 10 wt.% of the coating lost after drop tests. In most of the samples, the loss was around 5 wt.%. Thus, the "thin CNFs" are mechanically stable. The good attachment of CNFs is inherited from the excellent attachment of γ-alumina coating deposited on the stainless steel microreactor [19].

Experiments carried out with the bare microreactor without alumina coating yielded non-homogeneous and non-fibrous carbon deposits. This evidenced that the γ-alumina coating is

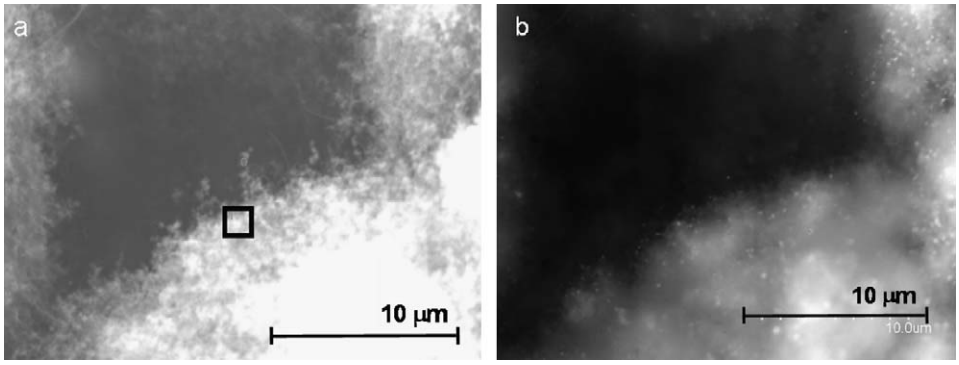

Fig. 9. SEM image representative of a region of "thick CNFs", which is magnification of spot 2 in Fig. 5. (a) SEM image recorded with secondary electrons; (b) SEM image recorded with backscattered electrons, where the brightest dots are catalyst metal particles.

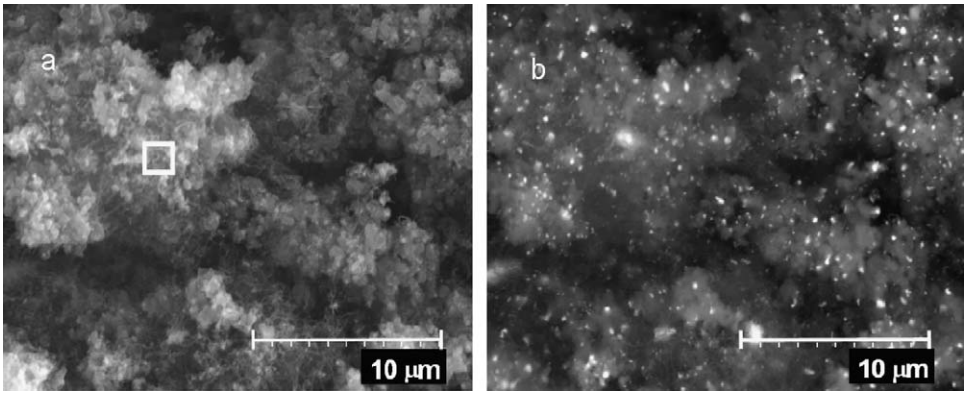

Fig. 10. SEM image representative of a region of "carbon protrusions", which is magnification of spot 3 in Fig. 5. (a) SEM image recorded with secondary electrons; (b) SEM image recorded with backscattered electrons, where the brightest dots are catalyst metal particles.

crucial for the yield of CNFs with uniform diameter. The γ-alumina coating ensures the dispersion of Ni catalyst to small particles with a narrow size distribution as observed by TEM (Fig. 9). Furthermore, sintering is prevented during the growth process. This is of paramount importance because it is reported that the CNF diameter is determined by the initial Ni particle diameter [20]. In the literature, CNFs have also been grown on stainless steel foils without alumina coating, after treating the stainless steel surface with an acid or base to induce fragmentation [21,22]. However, the CNFs had wider diameter distributions and less defined microstructure. Kiwi-Minsker and Tribolet [9] grew successfully uniform layers of CNF on stainless steel sintered metal fibers after oxidation in air at 550 °C. The small diameter of the fibers (about 35 μm) entails high surface area which can enhance the formation of metal nanoparticles from polycrystalline stainless steel. The metal nanoparticles are needed for the growth of CNFs. However, the lower surface area of microreactors and foils hinder the process of nanoparticle formation. This could explain the poor results when microreactors are not coated with alumina.

4. Conclusions

We have grown a uniform layer of entangled carbon nanofibers on stainless steel microreactors previously coated with Ni supported on γ-alumina layer. The mechanical stability of alumina coating was fundamental for the strong attachment of the subsequently grown CNFs. Besides, alumina coating ensured the growth of CNFs with uniform and thin diameter smaller than 50 nm. For the growth at the lowest temperatures, i.e. 853 and 873 K, CNFs smaller than 50 nm were the unique type of carbon present. In contrast, at growth temperatures exceeding 898 K, the carbon productivity increased dramatically but at the expenses of growing also non-filamentous carbon protrusions. These carbon protrusions plug the microreactor channels, rendering the microreactor unsuitable for a catalytic use.

The CNF coated microreactors prepared with methane at all temperatures and with ethane at temperatures under 873 K have good perspectives to be used in applications that can exploit the advantages of the association of CNFs as catalyst support and microreactors.

Acknowledgments

We are indebted to the Spanish Government for the financial support (PI CSIC 200780/010, MAT 2008-02365). I. Tacchini is acknowledged for the helpful discussions and assistance in the interpretation of SEM images.

References

[1] G. Kolb, V. Hessel, Chem. Eng. J. 98 (2004) 1.
[2] P.W.A.M. Wenmakers, J.v.d. Schaaf, B.F.M. Kuster, J.C. Schouten, J. Mater. Chem. 18 (2008) 2426.
[3] P. Serp, M. Corrias, P. Kalck, Appl. Catal. A: Gen. 253 (2003) 337.
[4] D.S. Su, X. Chen, G. Weinberg, A. Klein-Hofmann, O. Timpe, in: S.B.Abd. Hamid, R. Schlögl (Eds.), Angew. Chem. Int. 44 (2005) 5488.
[5] K.P. de Jong, J. Geus, Catal. Rev. Sci. Eng. 42 (2002) 481.
[6] R. Vieira, C. Pham-Huu, M.J. Ledoux, Chem. Commun. 9 (2002) 954.
[7] R. Vieira, M.J. Ledoux, C. Pham-Huu, Appl. Catal. A: Gen. 274 (2004) 1.

[8] M.K. van der Lee, A.J. van Dillen, J.W. Geus, K.P. de Jong, J.H. Bitter, Carbon 44 (2006) 629.
[9] P. Tribolet, L. Kiwi-Minsker, Catal. Today 105 (2005) 337.
[10] N. Jarrah, J. van Ommen, L. Lefferts, Catal. Today 79–80 (2003) 29.
[11] N.A. Jarrah, F.H. Li, J.G. van Ommen, L. Lefferts, J. Mater. Chem. 15 (2005) 1946.
[12] N. Jarrah, J. van Ommen, L. Lefferts, J. Mater. Chem. 14 (2004) 1590.
[13] E. Garcia-Bordeje, I. Kvande, D. Chen, M. Ronning, Adv. Mater. 18 (2006) 1589.
[14] P. Li, T. Li, J.H. Zhou, Z.J. Sui, Y.C. Dai, W.K. Yuan, D. Chen, Microporous Mesoporous Mater. 95 (2006) 1.
[15] K.M. de Lathouder, T. Marques Flo, F. Kapteijn, J.A. Moulijn, Catal. Today 105 (2005) 443.
[16] N. Ishigami, H. Ago, Y. Motoyama, M. Takasaki, M. Shinagawa, K. Takahashi, T. Ikuta, M. Tsuji, Chem. Commun. (2007) 1626.
[17] I. Janowska, G. Wine, M.J. Ledoux, C. Pham-Huu, J. Mol. Catal. A: Chem. 267 (2007) 92.
[18] R. Zapf, G. Kolb, H. Pennemann, V. Hessel, Chem. Eng. Tech. 29 (2006) 1509.
[19] P.A.R. Cebollada, E. García-Bordejé, Chem. Eng. J. 149 (2009) 447.
[20] D. Chen, K.O. Christensen, E. Ochoa-Fernandez, Z. Yu, B. Totdal, N. Latorre, A. Monzon, A. Holmen, J. Catal. 229 (2005) 82.
[21] C. Masarapu, B. Wei, Langmuir 23 (2007) 9046.
[22] C.E. Baddour, F. Fadlallah, D. Nasuhoglu, R. Mitra, L. Vandsburger, J.L. Meunier, Carbon 47 (2009) 313.